Lambeth, J. D., & Kamin, H. (1976) *J. Biol. Chem. 251*, 4299–4306.
Lambeth, J. D., & Kamin, H. (1977) *J. Biol. Chem. 252*, 2908–2917.
Lu, A. Y. H., & Coon, M. J. (1968) *J. Biol. Chem. 243*, 1331–1332.
Madystha, K. M., & Coscia, C. J. (1979) *J. Biol. Chem. 254*, 2419–2427.
Mason, H. S. (1958) *Science (Washington, D.C.) 125*, 1185–1188.
Masters, B. S. S., Kamin, H., Gibson, Q. H., & Williams, C. H., Jr. (1965) *J. Biol. Chem. 240*, 921–931.
Mayer, R. T., & Durrant, J. L. (1979) *J. Biol. Chem. 254*, 756–761.
Miyake, Y., Mason, H. S., & Landgraf, W. (1967) *J. Biol. Chem. 242*, 393–397.
Peisach, J., & Blumberg, W. E. (1970) *Proc. Natl. Acad. Sci. U.S.A. 67*, 172–179.
Sawada, Y., Iyanagi, T., & Yamazaki, I. (1975) *Biochemistry 14*, 3761–3764.
Siegel, L. M., Davis, P. S., & Kamin, H. (1974) *J. Biol. Chem. 249*, 1572–1586.
Sligar, S. G., Cinti, D. L., Gibson, G. G., & Schenkman, J. B. (1979) *Biochem. Biophys. Res. Commun. 90*, 925–931.
Taniguchi, H., Imai, Y., Iyanagi, T., & Sato, R. (1979) *Biochim. Biophys. Acta 550*, 341–356.
Vermilion, J. L., & Coon, M. J. (1974) *Biochem. Biophys. Res. Commun. 60*, 1315–1322.
Vermilion, J. L., & Coon, M. J. (1978a) *J. Biol. Chem. 253*, 2694–2704.
Vermilion, J. L., & Coon, M. J. (1978b) *J. Biol. Chem. 253*, 8812–8819.
Yasukochi, Y., & Masters, B. S. S. (1976) *J. Biol. Chem. 251*, 5337–5344.
Yasukochi, Y. Perterson, J. A., & Masters, B. S. S. (1979) *J. Biol. Chem. 254*, 7097–7104.

Computation of Enzyme–Substrate Specificity†

DeLos F. DeTar

ABSTRACT: The present study reports the development of a new procedure for the theoretical computation of enzyme–substrate specificities. The immediate goal has been to identify experimental data with which computations may be effectively compared, examine the underlying theoretical principles, and demonstrate feasibility. The experimental systems treated are hydrolyses catalyzed by chymotrypsin of Ac-Trp-NH_2, of Ac-Phe-NH_2, and of the Hein–Niemann "locked" substrate derived from phenylalanine; this may be designated as Lock-HN-OCH_3. For Trp and Phe, the L enantiomers are substrates while the D enantiomers are inhibitors, thus indicating differences of 7 kcal/mol or more in $\Delta\Delta G^{\ddagger}$ (D–L). For the "locked" substrate, the D enantiomer is the better substrate and $\Delta\Delta G^{\ddagger}$ (D–L) is −4 to −6 kcal/mol. We have used molecular mechanics to compute steric energies of models for the transition states for these hydrolyses and have been able to reproduce the experimental $\Delta\Delta G^{\ddagger}$ values surprisingly well even with a relatively primitive model. The differences in computed steric energies are not due to any one major term but are rather the consequences of summations of a large number of small terms. The new method shows promise of developing into a useful probe for the quantitative study of biochemical systems.

Many aspects of enzyme chemistry have been worked out in impressive detail. Yet one essential aspect has remained elusive: how to predict quantitatively the energies of interaction of substrates and enzymes so that analogous catalytic systems may be designed and synthesized at will. Such quantitative computational capability is likewise essential to the understanding of many other phenomena of biochemistry at the molecular level.

The size of enzyme molecules poses severe problems of logistics, and the need to obtain interaction energies to about 1 kcal/mol in order to predict rates even to a factor of 8 seems out of reach. However, we have in the past several years been employing the technique of molecular mechanics in a special way to estimate steric effects on reaction rates and have been able to estimate relative free energies of activation to about 0.5 kcal/mol in ester hydrolysis and in S_N2 cyclization reactions (DeTar & Tenpas, 1976; DeTar et al., 1978; DeTar & Luthra, 1980). It is promising, therefore, to apply this methodology to enzyme–substrate systems to see what sorts of results may be obtained.

Applications of molecular mechanics to problems of protein structure have a long history. Examples include prediction of conformations (Ramachandran et al., 1963; Scheraga, 1971; Momany et al., 1975; Momany, 1976; White & Morrow, 1977), estimation of energies of crystals of peptides and related molecules (Momany et al., 1974a,b; Hagler & Lifson, 1974; Hagler et al., 1974, 1976, 1979a–c; Hagler & Bernstein, 1978; Lifson et al., 1979; Dauber & Hagler, 1980), treatment of the complex problems of protein folding (Levitt, 1974; Honig et al., 1976; Levitt & Warshell, 1975; Finkelstein & Ptitsyn, 1977; Cohen & Sternberg, 1980; Lesk & Chothia, 1980; Hagler et al., 1979a–c), studies of ring conformations of proline (Ramachandran et al., 1970; Venkatachanlam et al., 1974, 1975; DeTar & Luthra, 1977, 1979), studies of binding of peptides to proteins (Platzer et al., 1972a,b; Bosshard, 1974; Pincus et al., 1976), and examination of protein dynamics as in the behavior of an internal aryl ring in interacting with a peptide system (McCammon & Karplus, 1979).

To calculate theoretically the rate of a reaction it is sufficient to calculate $\Delta G^{\ddagger}$, the free energy of activation. This can be represented as the difference in the free energy of formation of the transition state and of the reactant state. In particular it is not necessary to trace such details as reaction trajectories, nor is it necessary to take specific account of minor energy minima, identifiable experimentally perhaps as conformational

† From the Department of Chemistry, The Florida State University, Tallahassee, Florida 32306. *Received July 15, 1980.* This work was supported in part by generous grants of computing time by the Computing Center of the Florida State University as well as by the National Resource for Computation in Chemistry.

0006-2960/81/0420-1730$01.25/0

reorganization along the way to products or perhaps merely along dead-end byways.

We cannot usually predict absolute rates of reactions; our practical concern is with relative rates. For two reactants we therefore wish to evaluate theoretically some quantity $\Delta\Delta X$ which we expect will be equal to or proportional to $\Delta\Delta G^{\ddagger}$, the difference in $\Delta G^{\ddagger}$ values for the pair. In more general terms we wish to obtain a linear free energy relationship between $-RT \log k$ ($=\Delta G^{\ddagger}$) and the computed estimate ΔX in which the intercept may be arbitrary but the slope, which is the relationship between $\Delta G^{\ddagger}$ and ΔX, does not deviate too far from unity. Adjustment of the slope helps to compensate for minor deficiencies in the range of energies defined by a force field and for certain other minor effects on the energies of activation.

We intentionally imply that the proper test of a computational procedure requires the availability of a broad range of rate constants k against which to compare the computed quantities ΔX.

In order to make an estimate of $\Delta G^{\ddagger}$, we must identify appropriate components for which ΔX may be a suitable representation. To make the matter specific, we shall in the present study be interested in evaluating that part of enthalpy of activation that is due to steric effects, and we shall therefore consider ΔX to be primarily an enthalpic steric effect which can be calculated in terms of a suitable ΔSE, the steric energy difference. The steric energies SE are to be evaluated by molecular mechanics.

Returning to the general treatment, $\Delta\Delta G^{\ddagger}$ can be separated into an enthalpic term $\Delta\Delta H^{\ddagger}$ and an entropic term $T\Delta\Delta S^{\ddagger}$. We now consider their components.

The $\Delta\Delta H^{\ddagger}$ values may be dissected into four major terms (DeTar, 1980a,b). These are a bonding energy term, a polar term, a steric term, and a solvation term. The difference in rate of hydrolysis of an amide $RCONH_2$ and an ester $RCOOCH_3$ is due primarily to differences in bonding energy at the amide and ester functions and to corresponding differences in bonding energies of the transition states. The polar term serves to relate such rate differences as the 250-fold faster rate of alkaline hydrolysis of $ClCH_2COOC_2H_5$ than of $CH_3COOC_2H_5$ (DeTar, 1980a,b; Ashworth & Coller, 1971) to the 100-fold difference in acidity of the corresponding acids (Körtum et al., 1961). Steric effects and solvent effects will be considered more fully below. There is often interaction among these four terms; for instance, hydrolysis of an ester may have different solvation requirements than does hydrolysis of an amide.

Entropies may also be dissected into subcategories, with translation and overall rotation the largest contributors. Internal rotations, librations, and vibrations are the primary candidates for contributing to entropic differences among bound substrates whether complexed with enzyme but otherwise "free" or whether actually covalently bonded. The special motions of a "free" but complexed substrate may be considered as forms of libration.

In order to make headway in the theoretical computation of relative rates, it is essential to select a series of reactants for which one type of enthalpic term is dominant or else for which suitable corrections may be made for the effects of other terms. It is further necessary either to make a theoretical computation of the entropic terms or else to hope that for the substrates under study the $T\Delta\Delta S^{\ddagger}$ term is small compared to the $\Delta\Delta H^{\ddagger}$ term.

In the present study, we propose to compute substrate–enzyme specificities, particularly the steric aspects. We need therefore to consider briefly what sorts of steric effects are known. There are three general categories with indistinct boundaries. These are steric hindrance (DeTar & Tenpas, 1976; DeTar, 1980a,b), steric acceleration (DeTar & Luthra, 1980), and steric orientation. While all three steric factors may be involved in enzymatic catalysis, we expect that the most important is steric orientation; but it does not matter greatly whether we err in the identification, since the computational procedure we are using will include whatever steric effects may actually be present.

A theoretical understanding of enzyme–substrate and related interactions, the goal proposed in the opening paragraphs, requires development of reliable computational techniques for quantitative assessment of the subtle steric interactions involved. This component of the overall project is itself a long-range goal. The limited purpose of the present study is to define a promising new approach and to examine its feasibility.

Strategy for the Computations

Our first task was to select a suitable enzyme or suitable enzymes having as many as possible of the following characteristics: (1) The structure should be known by X-ray studies. (2) The enzyme should be active toward a range of substrates so that the computational approach can be tested adequately. (3) The mechanism should be understood so that observable rates and equilibria can be related to specific enzymatic steps and equilibria. (4) It would be convenient if the conformational changes are small as substrate is bound, since fewer conformational possibilities would then require evaluation.

α-Chymotrypsin and certain other members of the serine-protease family fulfill most of these desiderata. There are X-ray data for three chymotrypsin preparations (Steitz et al., 1969; Blow, 1976a,b; Birktoft & Blow, 1972; Rodgers et al., 1976; Henderson, 1970; Vandlen & Tulinsky, 1971, 1973a,b; Tulinsky et al., 1973, 1978; Cohen et al., 1969; Davies et al., 1969; Segal et al., 1971; Bernstein et al., 1977) and for chymotrypsinogen (Bernstein et al., 1977; Kraut, 1971, 1977; Birktoft et al., 1976; Matthews et al., 1977). There are difference X-ray studies for complexes with inhibitors and pseudosubstrates which show the probable positions assumed by substrates; these also show that binding causes few changes in the structure of the enzyme, at least for the crystalline enzyme (Blow, 1976a,b; Rodgers et al., 1976; Henderson, 1970; Tulinksky et al., 1978; Ruhlmann et al., 1973). Chymotrypsin is active with a broad range of substrates; the mechanisms have been investigated in great depth for some substrates (Bender & Killheffer, 1973; Hein & Niemann, 1962a,b; Zerner & Bender, 1964; Zerner et al., 1964; Kezdy et al., 1964; Bender & Kezdy, 1964; Bender et al., 1964; Komiyama & Bender, 1979; Brandt et al., 1967; Fastrez & Fersht, 1973; Foster & Niemann, 1955; Foster et al., 1955; Cohen & Schultz, 1968; Blow, 1976; Wallace et al., 1963). There are therefore many quantitative experimental data that can serve to evaluate the successes or failures of the computations.

Chymotrypsin has other useful characteristics. The active site region has an aryl pocket which largely envelops the side chain of the substrate. If the side chain is sufficiently large, then the possible conformations are restricted, thus simplifying the computational problems.

There are two reaction steps that may be expected to depend significantly on, and for some substrates primarily on, the energy of steric orientation. These are conversion of the complexed "free" substrate to tetrahedral intermediate on the way to acyl-enzyme (eq 1) and the corresponding formation

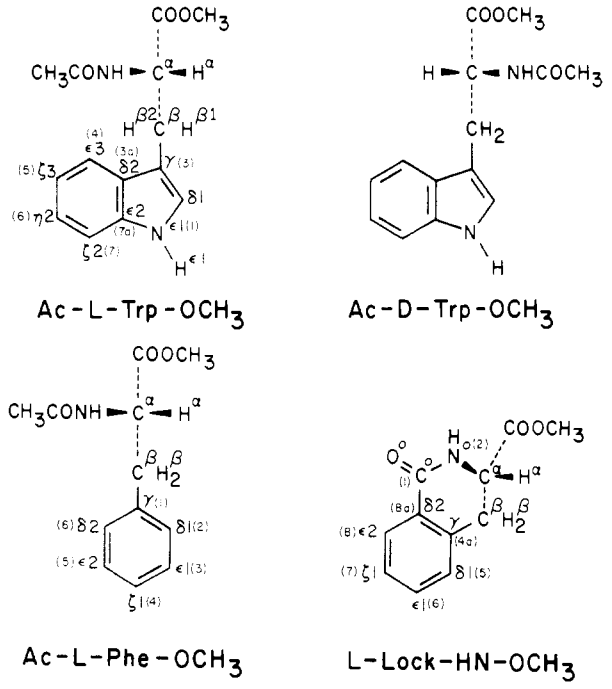

FIGURE 1.

of a somewhat different tetrahedral intermediate on hydrolysis of the acyl-enzyme (Kraut, 1977; Bender & Killheffer, 1973). The present modeling treats the acylation step, eq 1, and

$$\underset{\text{E–S complex}}{\text{RCOX·HOEnz}} \rightarrow \text{transition state} \rightarrow \underset{\text{acyl-enzyme}}{\text{RCOCEnz}} + \text{HX} \quad (1)$$

proposes to estimate $\Delta G^{\ddagger}$ on going from E–S complex to the transition state.

It is all important in these preliminary stages to seek out particularly clear-cut examples in order to ascertain whether the computational approach and the models are potentially useful. We have accordingly chosen three enantiomeric pairs of substrates for the computation: Ac-L-Trp-OMe, Ac-D-Trp-OMe, Ac-L-Phe-OMe, Ac-D-Phe-OMe, L-Lock-HN-OMe, and D-Lock-HN-OMe (see Figure 1). *Lock*-HN stands for the Hein–Niemann "locked" substrate derived from phenylalanine (Hein & Niemann, 1962a,b; Cohen & Schultz, 1968; Blow, 1976).

As a group these have several important characteristics. Ac-L-Trp-NH_2 is a substrate of chymotrypsin while the D enantiomer is an inhibitor (Foster & Niemann, 1955; Foster et al., 1955). The same is true for Phe. However, D-Lock-HN-OMe (related to Ac-D-Phe-OMe) is a better substrate than is the L enantiomer: the D/L $k_{cat}/K_{m\,app}$ ratio is about 1000–4000 (Hein & Niemann, 1962a,b; Cohen & Schultz, 1968). Since for the amides the acylation step is rate limiting, the observed rate constants pertain to acylation and the apparent K_m values are relatable to the dissociation constants for the E–S complex of eq 1 (Zerner & Bender, 1964; Zerner et al., 1964; Kezdy et al., 1964; Bender & Kezdy, 1964; Bender et al., 1964). For each D–L pair the K_m and K_I values are roughly equal (Foster & Niemann, 1955; Foster et al., 1955); for present purposes and probably within the limits of experimental measurement, we may take ΔG_f(D–L) = 0 for the E–S complexes. In the absence of an observable rate constant for the D isomer we can only set limits on the $\Delta\Delta G^{\ddagger}$(D–L). The k_L/k_D ratio presumably exceeds 10^5, and it may be larger. A reasonable expectation for $\Delta\Delta G^{\ddagger}$ is 7–9 kcal/mol, and in view of the $\Delta\Delta G_f$ (ground state) $\cong$ 0, this difference will arise primarily from a difference in $\Delta\Delta G_f$ of the transition states. It has been reported that formyl-D-Phe-OMe does turn over, that is, does show enzymatic catalysis and that ($k_{cat}/K_{m\,app}$) is of the order of 10^4 (L/D) (Hein & Niemann, 1962). The L–D discrimination appears greater for Trp than for Phe, and $\Delta\Delta G^{\ddagger}$(D–L) for Phe may be expected to be slightly smaller than for Trp, perhaps 6–8 kcal/mol.

The experimental situation has not been worked out for D- and L-Lock-HN-OMe. Usually methyl esters have the deacylation step rate limiting (Zerner & Bender, 1964; Zerner et al., 1964; Kezdy et al., 1964; Bender & Kezdy, 1964; Bender et al., 1964), and hence there is no direct relationship between $K_{m\,app}$ and the dissociation constant for the E–S complex. Inhibition constants have been reported for dozens of compounds; the range of values is rather narrow for compounds of analogous structure (Foster & Niemann, 1955; Foster et al., 1955; Wallace et al., 1963). The most reasonable assumption is that K_s, the dissociation constant for E–S complex, is comparable for the two enantiomers of Lock-HN-OMe and that $\Delta\Delta G_f \cong 0$. The ratio of $k_{cat}/K_{m\,app}$ values is then a measure of relative rate constants. The $\Delta\Delta G_f$(D–L) for the transition states may therefore be taken as about −4 to −6 kcal/mol.

We now go through the list of enthalpic terms to be sure what assumptions are being made and to evaluate their validity. (1) For each D–L pair the bonding terms are identical—amide vs. amide or ester vs. ester. These therefore cancel for an enantiomeric pair. (2) Polar terms are likewise identical between enantiomers. (3) Steric terms are different and are to be computed. (4) We assume that solvation enthalpies for an enantiomeric pair are effectively equal. As can be seen from Figures 2–5 the geometries are closely similar for the transition state models, particularly with respect to solvent exposure.

As for entropic differences, we find that the freedom of the substrate in the covalently bound transition state is severely limited. We present computations below on the steric energies for a model in which substrate has been forced down into the pocket by a few tenths of an angstrom. Energies go up rather rapidly and to nearly the same extent for the D- and L-Trp; there are perhaps significant differences in conformational space for enantiomers of Lock-HN while there are marginal differences for D- and L-Phe.

It is possible to set limits on the entropy differences by a simple computation. Rotational freedom is not available to complexed or combined substrate. Translational entropy of restricted movement of substrate in the specificity pocket cannot exceed that of free motion in the equivalent volume. An estimate based on $\Delta S = R \ln (V_2/V_1)$ then sets an upper limit since it includes rotation as well as translation. The smallest available volume is the molar volume of substrate in the crystal, roughly 200 cm^3 for Ac-Phe-NH_2 or Ac-Trp-NH_2. The volume of the specificity pocket is no more than twice as large. Therefore the maximum entropy available is of the order of R ln 2 or 1.4 cal deg^{-1} mol^{-1}. The difference in entropy between enantiomeric substrates is far smaller than this limit.

As for vibrational terms, there is little restriction to vibration for a complexed substrate. The energy cost of small excursions of atomic groups is small. The differential entropy effects between enantiomers will be smaller than the entropy effect on a single substrate.

Even with liberal assignments it is not reasonable to expect a value larger than 3 for the $\Delta\Delta S$(D–L) term, with $T\Delta\Delta S <$ 1 kcal/mol.

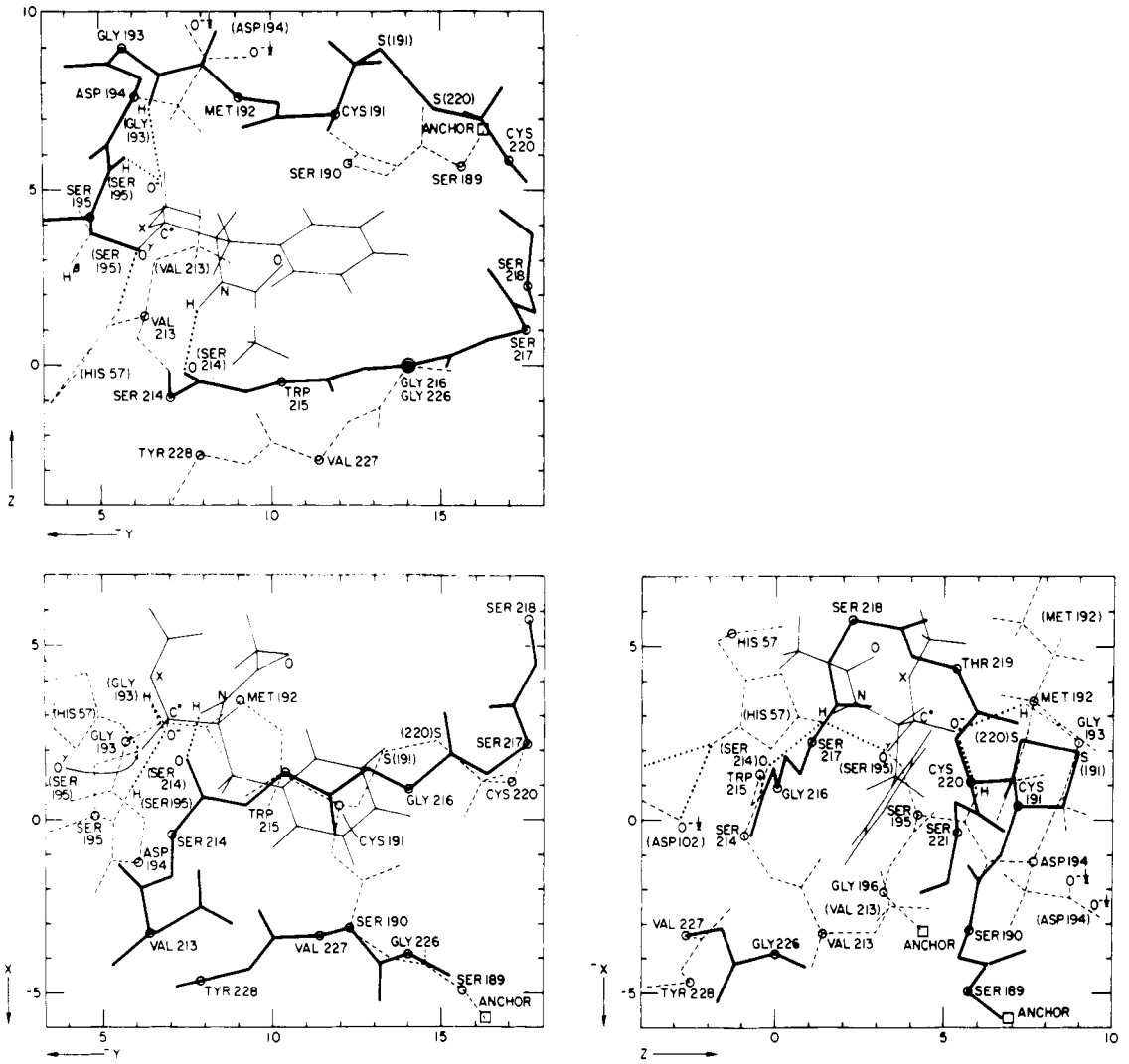

FIGURE 2: Ac-L-Phe-OCH_3 transition-state model with α-chymotrypsin active site. In Figures 2–5 the orthographic projections of models of the transition states (Table I) can be scaled to ascertain approximate locations of atoms. α-Carbon atoms are shown for each residue. Most side chains have been omitted in order to reduce clutter except for a few having special significance such as the CH_2–S–S–CH_2 linkage between C191 and C220, the side chain of Val_{213} that is near enough to interact with substrate, and the side chain of Asp_{194} that plays a critical role in forming the aryl pocket. Atoms at the tetrahedral center are labeled, C* for the carbon, O^-, O^γ of Ser_{195}, and X which is the oxygen of the OCH_3 group used in the model. Hydrogen bonds to substrate, or potential hydrogen bonds, are shown by dotted lines. The distance between C of Cys_{191} and C^α of Trp_{215} is taken as a measure of the size of the aryl pocket. These two atoms and C^β of Ser_{195} define a plane that is almost parallel to the *yz* plane in the figure. The top of the pocket lies roughly at $x = -2$ to $x = -3$ although Met_{192} forms a higher ridge at the Ser_{195} end. Except for L-Lock-HN the substrates treated in this study lie well down in the pocket. The deepest projection attained is $x = 2.6$ by $H^{\beta 3}$ (=H5) of Trp. The aryl ring of Tyr_{228} lies nearly parallel to the *yz* plane at $x = 6.5$, off scale to the bottom of the *xy* and *xz* projections. Although it, together with the side chain of Ser-190, appears to provide a well-defined bottom of the pocket, substrates apparently cannot penetrate deeply enough to interact with these side chains. Coordinates have been transformed from those reported by Birktoft and Blow (Birktoft & Blow, 1972); the transformation matrix is given in footnote 57 of DeTar (1981).

Models

The complexity of enzyme–substrate systems requires the development of simplified representations capable of reproducing the energies of interaction. We have examined the behavior of two models based on the 30 residues listed in Chart I. These include the active site and the specificity region and comprise about 15% of the enzyme. We have used the Birktoft–Blow coordinates for Ser_{195}-*O*-tosyl-α-chymotrypsin (Birktoft & Blow, 1972) but have added hydrogen atoms at standard positions.

In model 1 all 30 peptide residues were held at the reported X-ray coordinate locations although the side chains of certain residues and the substrate were relaxed (that is, positions of atoms were adjusted according to the force field). Chart I actually defines model 2 in which the peptide chain from Ser_{189}–Gly_{196} was relaxed, as were His_{57} and Asp_{102}.

Chart I

A. Residues Held at Birktoft-Blow Coordinates[a]
Ala_{55}-Ala_{56}-(His_{57})-Cys_{58}-Gly_{59}, Cys_{42}-Gly_{43}
Gly_{142}-Leu_{143}, Gly_{226}-Val_{227}-Tyr_{228}
Val_{213}-Ser_{214}-Trp_{215}-Gly_{216}-Ser_{217}-Ser_{218}-Thr_{219}-Cys_{220}-Ser_{221}

B. Residues Whose Positions Were Adjusted[b]
Ser_{189}-Ser_{190}-Cys_{191}-Met_{192}-Gly_{193}-Asp_{194}-Ser_{195}-Gly_{196}
anchored loosely at N of Ser_{189} and at C of Gly_{196}
His_{57} anchored by normal bonds to Ala_{56} and Cys_{58}
Asp_{102} anchored at N and C^α

[a] All hydrogen atoms were added, at standard tetrahedral geometries insofar as possible. [b] All hydrogen atoms were added.

The substrate models were represented by their methyl esters rather than as amides in order to provide some indication of the position assumed by a leaving peptide chain as modeled by the OCH_3 group. There is otherwise little difference be-

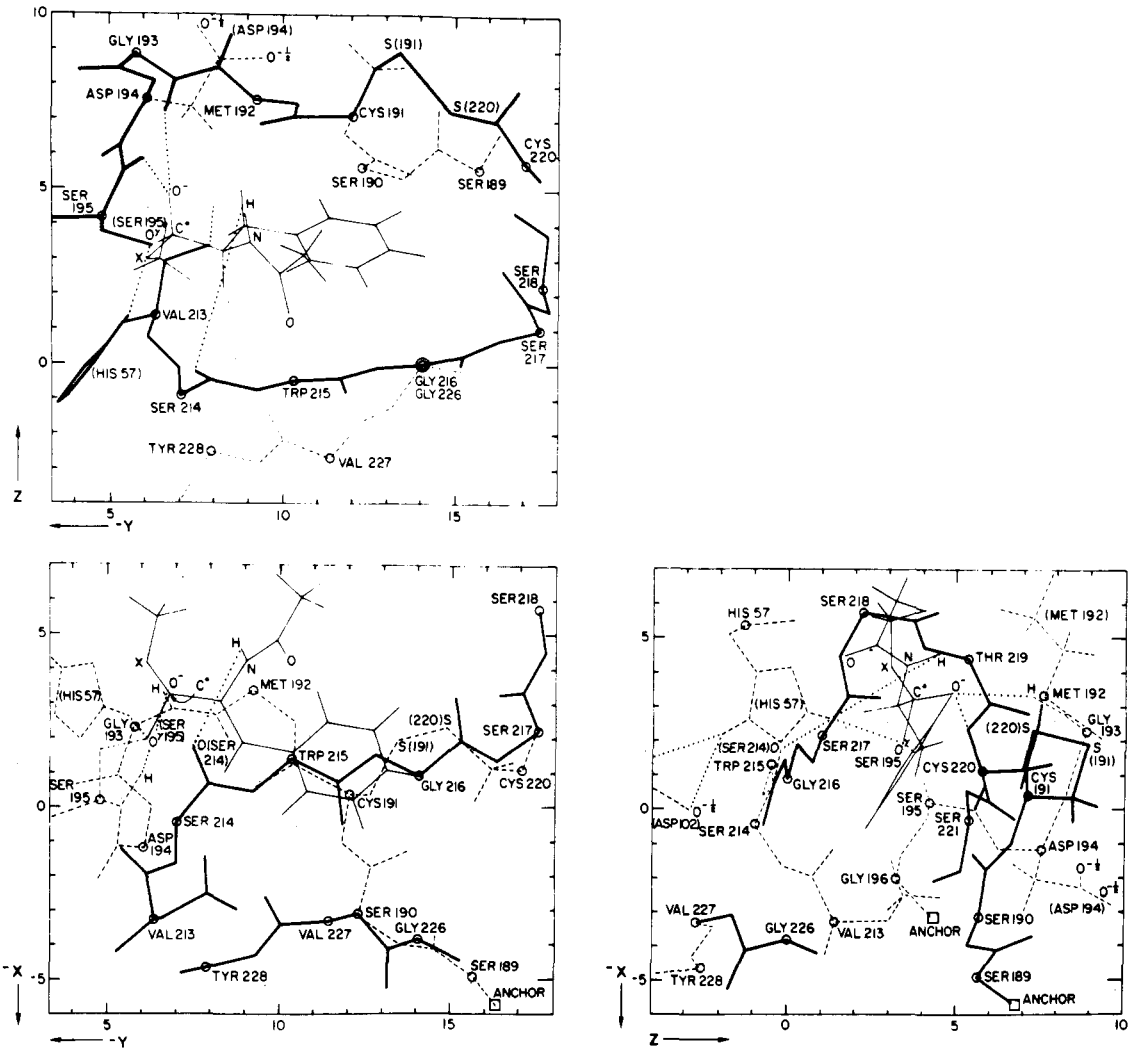

FIGURE 3: Ac-D-Phe-OCH_3 transition-state model with α-chymotrypsin active site. See Figure 2 for additional comments.

tween steric characteristics of an ester and an amide.

The transition state was represented as the tetrahedral intermediate: Ser-O^{γ}–C*(O^-)(OMe)R. It should be noted that these systems have a considerable flexibility. Although the O^{γ}–C* bond was treated as a normal bond, we do not expect computational results to be altered by choosing a longer bond. In a few computations the bond length was varied with only minor changes in energy.

Further details of the models are presented under Calculations and Results and Discussion and in the supplementary material (see paragraph at end of paper regarding supplementary material).

There are problems as to the best way to model dipolar and Coulombic interactions. These are of long range and of high energy in comparison to van der Waals interactions. The Coulombic effect of the included residues (Chart I) may not represent the effects present in the complete enzyme. At the same time total neglect is unrealistic. We have therefore adopted a compromise by including a specific set of important Coulombic interactions. The dipolar property of an amide group is represented by fractional point charges on the four atoms H—N—C=O, and the charges at the tetrahedral center are also represented by partial charges on four atoms O—C*—(O^-)—O. We included the interactions between two centers of substrate, namely, the tetrahedral center and the AcNH side chain, with three centers on the enzyme. Two of these are NH groups that hydrogen bond to O^-; they occur in the peptide bonds between Asp_{194}–Ser_{195} and between Met_{192}–Gly_{193}. The third involves the O of Ser_{214} which hydrogen bonds to the AcNH group of the L substrate (but not of the D); this occurs in the Ser_{214}–Trp_{215} peptide bond. These hydrogen bonds are shown in Figures 2–5. We included all 6 sets of these 16 pairwise point-charge interactions; either three (for the L enantiomer) or two (D) are strongly attractive while the remainder are neutral and serve to illustrate the general consequence of random long-range Coulombic effects.

We have also examined the effect of including all possible Coulombic charge interactions among the total 45 000 nonbonded interactions. The resulting D–L ΔSE values usually correspond quite well with those given by the simpler approximation, but there are also values that will require further examination.

Results and Discussion

Although we place no great faith in fine details of X-ray coordinates of large molecules, the Birktoft–Blow structure has received a great deal of qualitative study and merits a careful examination (Blow, 1976). We therefore wished to determine whether van der Waals repulsions applied to model 1 would serve to account for D–L differences. We examined Ac-Trp-OMe, Ac-Phe-OMe, and Ac-Ala-OMe and found very little ΔSE(D–L) difference for any D–L pair. The enzyme–

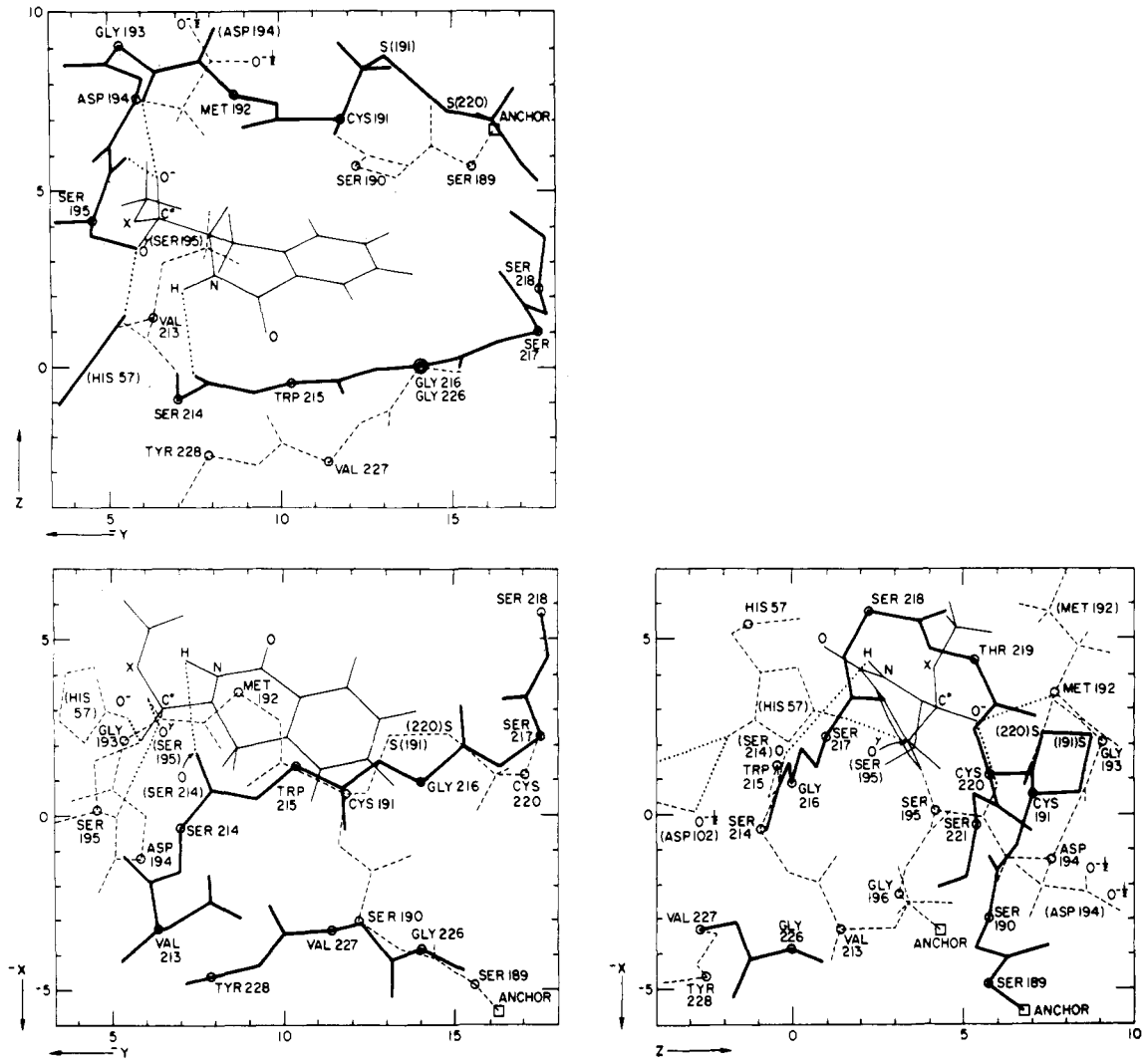

FIGURE 4: L-Lock-HN-OCH_3 transition-state model with substrate ring partly out of aryl pocket at α-chymotrypsin active site. See Figure 2 for additional comments.

substrate interaction is therefore unlike the situation in protein folding for which the van der Waals terms are often dominant. We do find differences for model 1 if the partial charges are included as is discussed under point 2 below.

We therefore turned to model 2 and in most studies we applied an arbitrary force across the pocket to cause it to close down on substrate and hence enhance the computed specificity. The peptide chain Ser_{189}–Gly_{196} is under control of the force field and can undergo those subtle modifications available to actual molecules. And the pocket can in fact close, as shown by the several X-ray studies (Vandlen & Tulinsky, 1973; Davies et al., 1969; Bernstein et al., 1977). Furthermore this chain reorganizes on conversion of chymotrypsinogen to chymotrypsin (Kraut, 1971, 1977). The closure process is therefore a physically realistic one. A possible function of the bulk of the enzyme may be to apply closure pressure across the specificity pocket.

The rest of this section is treated under nine topics: (1) overall energies obtained with model 2 and the best force field, (2) D–L differences with the Birktoft–Blow coordinates (model 1), with the partial Coulombic field, (3) the effect of variations of the force field on ΔSE values, (4) the question of multiple conformations, (5) geometrical results, (6) hydrogen bonds, (7) bond energy components of the steric energy, (8) nonbonded components of the steric energy, and (9) summary.

(1) The best values of the steric energies of the tetrahedral structures (transition-state models) are summarized in Table I, lines 1–4, and in Table IV. As can be seen from Table IV there is surprisingly good agreement with the experimental data. It is important to keep in mind that differences in steric energies are significant but that absolute values of steric energies are not.

The force field included a pocket restraint in the form of a Hooke's law function between C of Cys_{191} on one side of the pocket and C^{α} of Trp_{215} on the other, with a reference distance of 7.25 Å and a force constant of 1.44 kcal/Å. The effect of this function was to cause the distance between these two atoms to decrease from the 8.1 Å of the Birktoft–Blow study to about 7.5 Å. The rationale for this type of function has been presented above, and the effects of alternative choices are presented under point 3.

(2) The last two columns of Table II report the results for Ac-D-Trp-OCH_3 and Ac-L-Trp-OCH_3 based on model 1, all amino acid residues being held at the Birktoft–Blow X-ray position but with side chains of His_{57}, Asp_{102}, Met_{192}, Asp_{194}, and Ser_{195} relaxed. Several points are of importance: (a) The D–L difference is significant; it is about two-thirds as large as for model 2, Table I. (b) Most of the difference is due to the Coulombic terms. (c) It is obvious from the high steric energies that the X-ray coordinates include many bad local

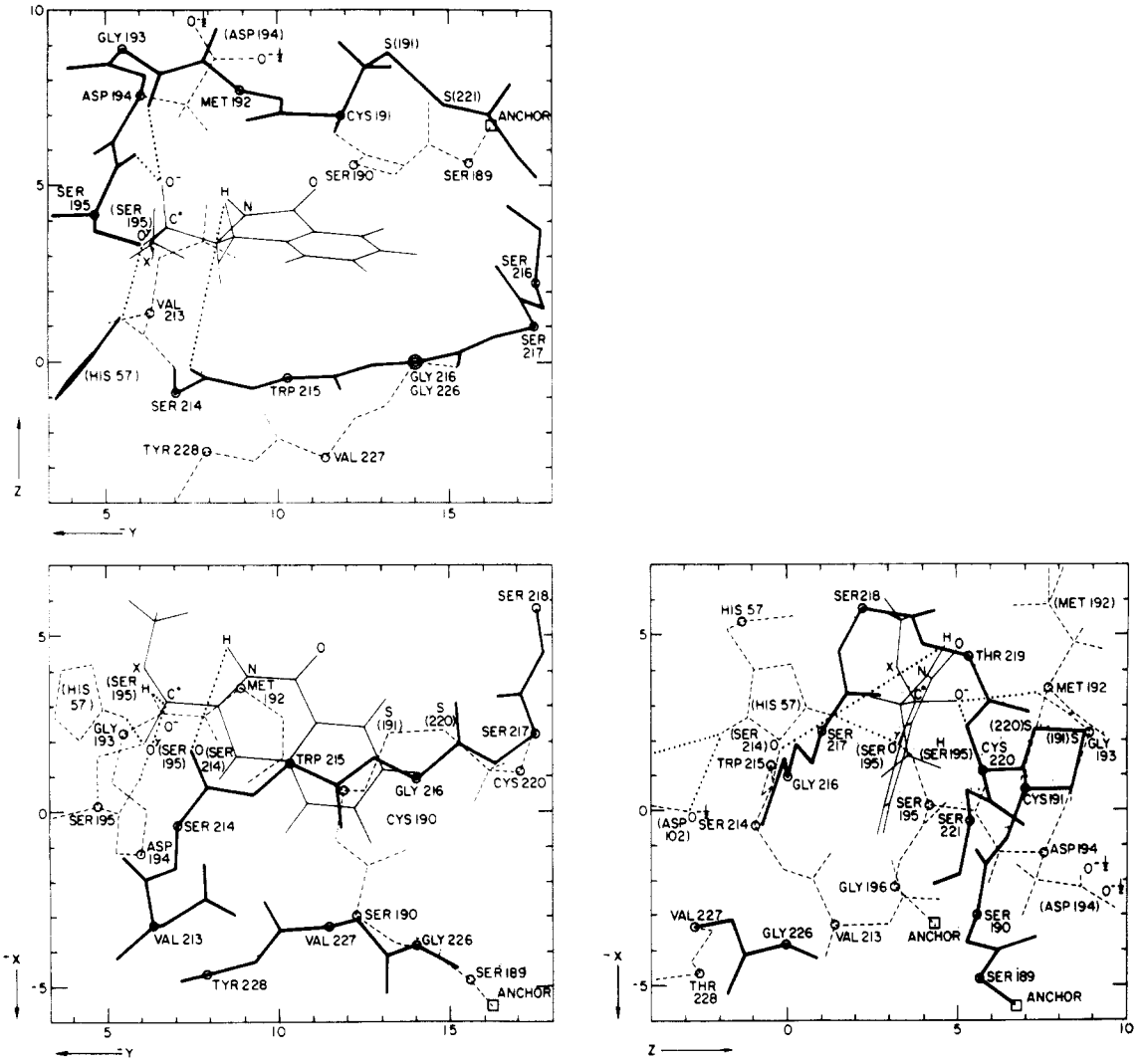

FIGURE 5: D-Lock-HN-OCH_3 transition-state model with α-chymotrypsin active site. See Figure 2 for additional comments.

geometries. These can be relieved by quite minor adjustments of a few angles and torsions. In fact, the absolute steric energies here are some 110 kcal more positive than for model 2. In spite of these large differences in individual SE values, the ΔSE(D–L) is within 2.5 kcal of the best value.

(3) Of central importance is the sensitivity of the computed ΔSE values to the constants of the force field. We find the ΔSE differences are relatively insensitive to the force field and illustrate this point with the data in Tables II and III.

The aryl pocket extends, apparently, to a far greater depth than is reached by the tosyl group in the X-ray study or by several substrates in the calculation reported in Table I and illustrated in Figures 2–5. We therefore looked at the consequences of forcing substrate deeper into the pocket by applying a pull-down force. There is no entirely satisfactory way to apply the same pull down to substrates of different structures, and the results in Table II must be evaluated pairwise. The position of substrate is indicated approximately by the x coordinate of C^γ, the positive x direction being toward bottom of the pocket. This coordinate is reported for the several computational variations, Tables I–III.

The pull-down value used for Trp caused a downward movement of about 0.15 Å at an energy cost of about 2 kcal/mol and with a D–L steric energy difference about 0.7 kcal/mol greater than before. The pull-down used for Lock-HN cost very little energy and brought the L-Lock-HN ring into a more normal conformational position than was obtained in the computation in Table I. Again the D–L energy difference is about the same as in Table I. The pull down used for Phe was clearly excessive in comparison with that used for the other two substrates. The phenyl ring of the Ac-L-Phe-X (tet) can slip at a canted angle into the pocket while such a special location is not available to the other substrates. However, even this much of the change resulted in but a 3 kcal/mol increase in the D–L steric energy difference.

In Table III we summarize the consequences of drastically clamping the pocket onto the substrate. These also are model 2 calculations, Chart I. The pocket width, defined as the distance between C of Cys_{191} and C^α of Trp_{215}, has been decreased from the 8.1 Å of the Birktoft–Blow coordinates and the 7.4–7.5 Å of the model of Table I down to 6.0 Å. It was also necessary to apply a pull-down force to keep the substrate from moving out of the pocket. This unreasonable force field results in a number of repulsive van der Waals contacts between substrate ring and both sides of the aryl pocket. The D–L steric energy differences ΔSE with this relatively drastic version of the force field have increased by 3.5 kcal/mol for Trp and decreased by about 2 kcal/mol for Lock-HN. That is, crowding the substrate increases the discrimination modestly. For each substrate, the total "strain" has increased by

Table I: Energies and Geometrical Parameters for Transition-State Model (Tetrahedral Intermediate) (No Pull-down Restraint)

	Ac-L-Trp-X	Ac-D-Trp-X	Ac-L-Phe-X	Ac-D-Phe-X	L-Lock-HN	D-Lock-HN
bond energy	17.7[a]	18.4	17.9	17.6	17.1	20.3
total NB energy	−128.8[b]	−122.3	−123.3	−117.1	−111.9	−116.3
net steric energy (SE)	−111.1	−104.0	−105.3	−99.5	−94.8	−96.2
ΔSE (D − L)	7.2		5.9		−1.4	
bond components[a]						
-substrate	5.5	5.8	5.9	5.2	5.3	7.7
-enzyme	12.2	12.5	12.0	12.4	11.8	12.7
NB components[b]						
-sub-sub	3.6	3.6	3.9	3.4	4.3	4.1
-sub-enz[c]	3.1	2.6	2.2	2.4	1.8	2.6
-enz-enz	21.6	22.6	20.9	22.1	20.3	21.6
M192 G193-tet[d]	−5.3	−5.5	−5.3	−5.4	−5.2	−5.4
D194 S195-tet[e]	−5.3	−3.5	−5.1	−3.9	−5.4	−4.5
M192 G193-amide	−0.1	0.2	−0.1	0.2	0.0	0.0
D194 S195-amide	−0.1	0.1	−0.1	0.1	0.0	0.0
S214 W215-tet[f]	0.7	0.8	0.7	0.8	0.7	0.8
S214 W215-amide	−1.8	0.0	−1.8	0.1	−0.6	−0.1
pocket restraint[g]	0.3	0.6	0.5	0.6	0.2	0.4
anchor[h]	1.6	2.0	1.7	1.6	1.2	1.0
vdW attraction[i]	−147.3	−145.8	−140.7	−138.8	−129.4	−136.7
geometric factors						
x coord for C^{γ} of sub	−1.584	−1.810	−1.148	−1.696	−3.010	−1.536
aryl pocket width[g]	7.460	7.542	7.502	7.541	7.422	7.477
H-bond distances						
S214 O–HN substrate[f]	2.294	(5.739)	2.225	(5.74)	(3.783)	(5.774)
S195 NH–O^- substrate[d]	2.127	3.003	2.106	2.832	2.173	2.581
G193 NH–O substrate[e]	2.251	2.302	2.234	2.296	2.179	2.255
H57 NH^{ϵ}–O^{γ} S195	2.109	2.259	2.017	2.173	2.069	2.165

[a] Energies in kcal/mol, distances in Å. See Figure 1 for structures; includes steric energies for all angles and torsions. [b] Total for some 45 000 nonbonded interactions. The component nonbonded terms are also itemized. [c] About 40% of the repulsion interaction is due to the aryl pocket. Most of the nonbonded repulsive terms involve the tetrahedral carbon atom and the four atoms attached. [d] Coulombic interaction involving the H bond between O^- of the transition state and Gly_{193} NH. [e] H bond between O^- of transition state and Ser_{195} NH. [f] H bond NH of AcNH of substrate and O of Ser_{214}. [g] Force constant of 1.44 kcal/Å and reference distance of 7.25 Å between C of Cys_{191} and C^{α} of Trp_{215}. The distance between those two atoms is defined as the pocket width. [h] Energy due to movement of Ser_{189}–Gly_{196} chain ends from X-ray anchor positions. [i] Sum of all the itemized nonbonded component terms equals the total NB energy. vdW = van der Waals.

about 30 kcal/mol, and there has even been a substantial distortion of one of the amide ω torsions (Cys_{191}) of the peptide chains. Even so, the computed D–L steric energy differences remain in reasonable and reasonably constant range. Clearly the computed results are insensitive to the several variations. These provide a relatively general test since they bring into play a large range of other force constants as many angles and torsions become strained.

These several results are entirely consistent with those obtained in many other molecular mechanics studies: although absolute values of steric energies are strongly dependent on details of the force field, differences in steric energies are relatively insensitive (DeTar & Tenpas, 1976; DeTar, 1980a,b; DeTar & Luthra, 1980; Bingham & Schleyer, 1971; Engler et al., 1973; Jacob et al., 1967; Thompson, 1967). In our experience nearly any reasonable force field consistently applied will give useful ΔSE values.

The steric energies resulting from these several different force fields are summarized in Table IV.

(4) We now address the question of multiple minima. In preliminary computations on "free" complexed substrates we have sought and have found clear examples of multiple minima. As another example, we were concerned about the rather strange conformation assumed by L-Lock-HN (Figure 4) and sought plausible alternatives. One energetically possible conformation has the ring system rotated nearly 180° with the amide side down, but this minimum may be ruled out because it has a higher energy and because the ring extends rather far out of the pocket. Another conformational minimum can be achieved through assigning alternative torsional values to the Ser_{195} O^{γ}–C(substrate) bond and the following bond, but this conformation places the O^{γ} near Asp_{194} and far from His_{57}, thus making the critical proton transfer impossible. These several examples show that we can locate alternative minima by examining physical models.

With the tetrahedral intermediates, the dual requirements of attachment to the O of Ser_{195} and of placing the aryl ring in the specificity pocket strongly limit conformational possibilities. In all the examples we have explored, there is a single conformation of minimum energy. It would be a rather costly program to undertake a systematic stepwise exploration; at best such a study might locate minima separated by shallow and insignificant barriers. In the several cases we have investigated, we have found that structurally perturbed conformations return to the earlier conformational minima when the original force field was restored.

There are conformational minima of low energy in which the aryl ring of the substrate is entirely out of and away from the aryl pocket. Such out-of-pocket conformations of acyl-enzyme or of tetrahedral intermediate cannot be reached by normal enzymatic catalysis involving prior complexation, but they could result from direct intermolecular (bimolecular) reaction. The entropic term for the intermolecular reaction makes this type of reaction highly unfavorable and these conformations unproductive.

Attention had to be paid to minor conformational variants. For example, the side chain of Met_{192} can achieve more than one conformation, and these differ among themselves by about 1.7 kcal/mol. It was therefore necessary to make sure that all computations used the same conformation here, namely,

Table II: Energies and Geometrical Parameters for Transition-State Model (Tetrahedral Intermediate) (with Pull-down Restraint)

	Ac-L-Trp-X	Ac-D-Trp-X	Ac-L-Phe-X	Ac-D-Phe-X	L-Lock-HN	D-Lock-HN	Ac-L-Trp-X	Ac-D-Trp-X
bond energy	18.1	18.7	19.0	18.4	19.9	20.6	52.3	52.8
total NB energy	−127.3	−120.0	−120.8	−111.0	−114.1	−116.7	−50.6	−46.3
net steric energy	−109.2	−101.3	−101.8	−92.6	−94.1	−96.2	1.7	6.5
ΔSE (D − L)	7.9		9.1		−2.0		4.8	
bond components[a]								
substrate	5.6	5.9	6.5	5.6	7.0	7.8	5.6	6.6
enzyme	12.5	12.8	12.5	12.8	13.0	12.8	46.6	46.2
NB components[b]								
sub-sub	3.6	3.7	4.0	3.3	4.9	4.2	3.3	3.4
sub-enz[c]	3.0	3.3	2.4	2.7	2.6	2.7	4.1	4.5
enz-enz	22.1	23.4	21.3	22.5	21.1	21.2	96.2	96.5
M192 G193-tet[d]	−5.3	−5.4	−5.2	−5.4	−5.2	−5.4	−4.6	−3.7
D194 S195-tet[e]	−5.2	−3.5	−5.0	−3.9	−5.0	−4.6	−5.3	−4.1
M192 G193-amide	−0.1	0.2	−0.1	0.2	0.0	0.0	−0.1	0.2
D194 S195-amide	−0.1	0.1	−0.1	0.1	0.0	0.0	−0.1	0.1
S214 W215-tet[f]	0.6	0.8	0.6	0.8	0.7	0.7	0.6	0.7
S214 W215-amide	−1.8	0.0	−1.8	0.0	−0.7	−0.1	−1.5	0.0
pocket restraint[g]	0.3	0.6	0.4	0.8	0.3	0.4		
pull-down restraint	1.7[j]	2.3[j]	3.3[k]	6.2[k]	0.5[l]	0.1[l]	*m*	*m*
anchor[h]	1.5	1.9	1.8	1.6	1.5	1.1		
attraction[i] vdW	−147.7	−147.4	−142.2	−139.9	−134.9	−137.0	−143.1	−144.0
geometric factors								
x coord for C^{γ} of sub	−1.418	−1.571	−0.591	−1.219	−1.642	−1.419	−1.356	−1.388
aryl pocket width[g]	7.467	7.549	7.488	7.580	7.464	7.480	8.09	8.09
H-bond distances								
S214 O–HN substrate[f]	2.271	(5.657)	2.246	(5.618)	(3.505)	(5.749)	2.561	(5.972)
S195 NH–O^- substrate[d]	2.114	2.990	2.089	2.811	2.079	2.538	2.162	2.709
G193 NH–O^- substrate[e]	2.284	2.384	2.272	2.353	2.241	2.264	2.561	2.972
H57 NH^{ϵ}–O^{γ} S195	2.167	2.301	2.086	2.200	2.079	2.162	2.632	2.659

[a–i] See Table I. [j] Pull-down 2.9 kcal $Å^{-2}$ mol^{-1} for all; reference 5.0 Å to C^{ϵ_2}. [k] Reference 6.0 Å to C^{γ}. [l] Reference 7.0 Å to C^{β}. [m] No pull down, no pocket restraint, main chain held at X-ray coordinate positions.

Table III: Energies for Transition-State Models with Strong Constriction of Aryl Pocket

	Ac-L-Trp-X	Ac-D-Trp-X	L-Lock-HN	D-Lock-HN
bonded	29.8	31.0	34.9	34.2
total nonbonded	−109.0	−99.5	−101.2	−104.0
net steric energy	−79.2	−68.5	−66.3	−69.7
SE difference	10.7		−3.5	
pocket width	6.036	6.034	6.034	6.028
x coord C^{γ}	−1.248	−1.564	−1.464	−1.649

[a] Pocket forced to close with reference distance between C of Cys_{191} and C^{α} of Trp_{215} of 6 Å and force constant of 1400 kcal/Å. Pull-down force 5 times stronger than for runs in Table II, same reference distances.

the roughly all-*s*-trans conformation.

The enzyme chain Ser_{189}–Gly_{196} is relatively stable to conformational changes under the anchoring conditions used in the model. None of the distortions reported under point 2 nor any of the even more drastic distortions we tested caused the enzyme chain to jump into an alternate conformation that used significantly different ϕ–ψ angles. We were able in some cases to get conformers differing by a few degrees in certain angles on either side of a low eclipsing barrier. We do not mean to imply that the peptide chain is rigid; it is not. But we did not find any deep multiple minima as the several torsions and bonds underwent accommodations from one substrate to another.

(5) Geometrical results for Phe and for Trp show significant similarities, and D and L geometrical differences tend to be parallel. Examples are Ser_{195}-O^{γ}–C*–C^{α}–N(substrate), the torsion which determines the position of the AcNH side chain. Values are 136 (D) vs. 233 (L) for Phe and the parallel values of 136 (D) vs. 236 (L) for Trp. For the L substrates the AcNH group is rotated so as to H-bond to the O of the Ser_{214}. For the D substrate the AcNH group has to be rotated out of pocket to minimize unfavorable van der Waals contacts with the H^{α} and an H^{γ} of Met_{192}. Other parallel D–L differences involve the substrate attachment sequences: Ser_{195} C^{α}–C^{β}–O^{γ}–C*(substrate) 141 (D) vs. 107 (L) Phe, 148 (D) vs. 113 (L) Trp; C–C^{α}–C^{β}–C^{γ}(substrate) 175 (D) vs. 166 (L) Phe, 162 (D) vs. 154 (L) Trp; C^{α}–C^{β}–C^{γ}–C^{δ}(substrate) 291 (D) vs. 330 (L) Phe, 304 (D) vs. 345 (L) Trp; position of CH_3O of substrate: Ser C^{β}–C^{γ}–C*–O (of OCH_3) 129 (D) vs. 146 (L) Phe, 127 (D) vs. 138 (L) Trp. A further 10 torsions show differences of 5 to 10° while the remaining torsions are the same within 5° or less. These analyses illustrate the structural consistencies of the computations.

Another geometrical factor of interest is the position of the substrate with respect to the "top" of the aryl pocket. Although "top of pocket" cannot be defined precisely, as is clear from Figures 2–5, the triplet of atoms consisting of the C of Cys_{191}, C^{α} of Trp_{215}, and C of Ser_{195} defines a plane that is nearly parallel to our *yz* plane at $x = -1.35$ A. The positive *x* direction points to the bottom of the pocket. The *x* values reported for C^{γ} of substrate in Tables I and II mostly place this atom slightly above this plane. Figures 2–5 provide further

Table IV: Summary of Component D–L Differences in Steric Energies for Model of Transition State for Acylation Step[a]

	Ac-Trp-X[b]	Ac-Phe-X[c]	Lock-HN[c]
experimental $\Delta\Delta G$	7–9	6–8	−4 to −6
calculated ΔSE	7.2, 7.9, 4.8	5.9, 9.1	−1.3, −2.0
components of ΔSE			
H bond AcNH to O of S214	1.8, 1.8, 1.5	1.8, 1.8	(0.6), (0.6)
H bond O^- to NH G193	−0.2, −0.1, 1.0	−0.2, −0.1	−0.2, −0.2
H bond O^- to NH S915	1.8, 1.7, 1.2	1.3, 1.2	0.9, 0.4
other Coulombic	0.6, 0.6, 0.6	0.6, 0.6	0, 0.1
bond ΔSE	0.7, 0.6, 0.6	−0.3, −0.6	3.2, 0.6
pocket restraint, anchoring pull-down	0.7, 1.4, 0	0, 3.1	0, −0.8
repulsion vdW	0.4, 1.6, 0.9	0.8, 0.9	1.8, −0.6
attraction vdW	1.5, 0.2, −1.0	1.9, 2.3	−7.3, −2.1
subtotal[d]	3.3, 3.8, −0.1	2.4, 5.7	−2.3, −2.9

[a] All energies kcal/mol. [b] First entry is from Table I; second entry is from columns 1 and 2 of Table II; third entry is from last two columns of Table II. [c] First entry is from Table I; second entry is from Table II. [d] Sum of bond ΔSE, pocket restraint, etc., and vdW repulsion and vdW attraction.

Table V: Status of Torsions in the Enzyme Main Chain

		Ac-L-Trp-OCH_3		Ac-D-Trp-OCH_3	L-Lock-HN	
		Table II[a]	Table I	Table I	Table I	Table III
G196	ϕ	91.1	88.6	92.0	86.4	88.1
Ser_{195}	ϕ	303.7	316.2	319.9	314.7	302.0
	ψ	140.6	110.7	107.1	108.8	115.2
	ω	180.5	183.4	182.8	182.8	181.7
Asp_{194}	ϕ	278.9	301.1	302.3	298.5	298.2
	ψ	336.2	331.9	333.5	336.3	338.7
	ω	182.3	185.0	180.6	186.4	192.3
Gly_{193}	ϕ	107.9	91.0	90.1	89.8	92.2
	ψ	335.4	318.7	320.1	317.3	311.5
	ω	179.4	175.3	173.0	178.2	181.4
Met_{192}	ϕ	294.3	307.5	310.0	307.4	316.1
	ψ	133.6	140.0	141.2	148.2	139.1
	ω	176.4	177.1	176.9	179.5	174.3
Cys_{191}	ϕ	228.7	208.4	210.7	208.4	206.1
	ψ	192.1	187.0	180.1	179.3	189.6
	ω	173.7	171.1	174.9	172.5	139.5
Ser_{190}	ϕ	297.2	292.3	294.6	291.0	286.7
	ψ	156.3	171.3	165.8	164.9	175.5
	ω	175.9	188.7	189.1	185.8	192.3
Ser_{189}	ψ	289.7	289.5	289.4	290.8	291.2
	ω	163.5	175.4	174.8	178.7	176.7
pocket width C(C191)–C^α(W215)		8.1	7.45	7.52	7.42	6.03

[a] X-ray values (degrees).

illustrations as does the figure in DeTar (1981).

We comment briefly on one other structural aspect of the Birktoft–Blow structure. The side chain of Tyr_{228} appears to be able to hydrogen bond to the side chain of Ser_{190} to form a clearly defined bottom for the aryl pocket, but this bottom is quite deep and none of the substrates has gotten closer than about 4 Å.

Table V summarizes the changes in torsions for the enzyme chain as the pocket size is changed and as representative substrates are accommodated. At the 7.4–7.5-Å pocket size (specified on the bottom line) the differences are minor for different substrates. The major change on reducing the pocket size to 6 Å is a severe distortion of ω for Cys_{191}.

Table VI summarizes angles and torsions for the saturated ring of Lock-HN. The reversal at C^α–C^β–C^γ–$C^{\delta'}$ represents

Table VI: Angles and Torsions for Lock-HN Ring for Transition State Model

	L[a]	L[b]	D[b]
C^*–C^α–C^β–C^γ	172.0	177.4	169.1
C^α–C^β–C^γ–C^{δ_1}	211.1	217.4	154.9
C^α–C^β–C^γ–C^{δ_2}	31.1	37.4	334.9
C^β–C^γ–C^{δ_2}–C^o	13.4	4.7	351.3
C^γ–C^{δ_2}–C^o–N^o	334.3	336.0	18.6
C^{δ_2}–C^o–N^o–C^α	348.9	357.4	8.6
C^o–N^o–C^α–C^β	60.0	44.3	319.0
N^o–C^α–C^β–C^γ	298.2	301.4	47.1
C^α–C^β–C^γ	108.2	108.9	113.6
C^β–C^γ–C^{δ_2}	120.0	120.0	120.0
C^γ–C^{δ_2}–C^o	116.0	116.3	118.2
C^{δ_2}–C^o–N^o	113.8	114.8	115.4
C^o–N^o–C^α	112.2	124.2	125.3
N^o–C^α–C^β	104.3	106.3	108.4
C^β–C^γ–C^{δ_2}	120.0	120.0	120.0

[a] With pull-down force, Table II. [b] No pull-down force, Table I.

mirror image deviations from a 180° mean. There are small deviations from planarity across the amide bond and across the ortho position of the ring. The two conformations for L-Lock-HN-OCH_3 transition state illustrate the deviations that accompany the fitting of a substrate into a specific enzyme site.

(6) Hydrogen bonds all form as expected. This is, of course, primarily a consequence of staying close to the X-ray coordinates. Hydrogen bonds are indicated by dotted lines in Figures 2–5. There are, however, some important differences between enantiomers. The most famous H bond is that involved in the serine to histidine transfer, a critical step in the catalytic process. In our model of the transition state this hydrogen has been transferred to the imidazole ring of His_{57} and the significant hydrogen bond is therefore from NH^δ to Ser_{195} O^γ. The hydrogen bond distances for this pair are summarized in Tables I and II; all are about 2 Å. The other hydrogen bond of the "charge relay" system is, in the present model, between the $NH^{\epsilon 2}$ and an oxygen of the β-carboxylate group of Asp_{102}. This distance was about 2.5 Å throughout and was constrained primarily by our use of the X-ray coordinates to anchor the Asp_{102} while His_{57} was anchored into the Ala_{56}–Cys_{58} sequence. Hydrogen bonds from the O^- of the tetrahedral center to the NH of Ser_{195} and the NH of Gly_{193} are a significant factor in the D–L energy differences (Tables I–III).

(7) Although details of energy values will differ with differing models and differing force fields, it is instructive to make internal comparisons to ascertain what factors are involved. Bond energy components are itemized as those due to substrate and those due to enzyme; they are "strains" which arise from angles and torsions which differ from reference values. It is usually not possible to pinpoint the cause of the strain. Even for D-Lock-HN, which has a substrate bond energy some 2.3 kcal higher than does the L enantiomer, the precise origins of differences are obscure; some 20 angles and torsions have slightly higher values for the D enantiomer. The effect is centered on the tetrahedral carbon which has bonds and torsions that are a bit farther off of standard for the D than for the L enantiomer. No one or two values is clearly different.

(8) Nonbonded van der Waals repulsive interactions control much of the geometry. Slightly larger enzyme–enzyme repulsive interactions for the D isomers account for about 1 kcal/mol of D–L differences for Trp and for Phe. Substrate–substrate repulsive interactions and a significant part of the substrate–enzyme repulsive interactions are due to the

expected crowding at the tetrahedral center (DeTar & Tenpas, 1976). It is interesting to note that repulsive interactions in the aryl pocket are small for all models reported in Tables I and II. The origins of the principal pocket repulsions may be summarized as follows: H^{α} of Cys_{191} interacts with ring atoms C^{ϵ} of Phe and N^{ϵ} of Trp; O of Cys_{191} interacts with one of the H^{β} of the substrate; H^{α} of Met_{192} interacts with H^{β} of substrate for the D enantiomers; H^{α} of Gly_{216} interacts with the aryl rings—with C^{ϵ_1} and H^{ϵ_1} of Phe and with C^{η} of Trp. Other interactions occur for some substrates. Repulsive interactions between the H of AcNH of D substrate with H^{α} and H^{γ} of Met_{192} were mentioned above. Individually these interactions represent very little energy, but they flag the fact that adjustments were not able to entirely eliminate certain repulsive interactions.

The van der Waals (vdW) attractive component appears to play a significant role for these models. The individual pairwise vdW terms are small, the average being less than 0.003 kcal/mol, but the overall effect of some 45 000 terms bears a significant relationship to how far the substrate extends into the aryl pocket. For example, the L-Lock-HN does not fit very well and rides up out of the pocket by about 1.4 A as indicated by the x-coordinate value (Table I). This results in a reduced attractive van der Waals component by some 7 kcal/mol in comparison to the D enantiomer. On these grounds the D enantiomer becomes favored even though several other smaller terms favor L over D as is the pattern for Phe and Trp.

Similar considerations also hold for the other D–L pairs, but to a smaller extent. van der Waals attraction contributes about 1.5 kcal or more to the D–L difference. In every case the better substrate tends to fit deeper into the aryl pocket.

(9) In summary, Table IV provides an overall summary of the computational results. The first entry in each column is derived from Table I and compares computations based on exactly the same force field for every substrate. The second entry in each column is derived from the first six columns of Table II. The force field is the same as for runs of Table I except that a pull-down force has now been added; the pull-down is necessarily different for each substrate because of differences in geometry. The third entry for Ac-Trp-X summarizes the last two columns of Table II; the enzyme main chain was held fixed at the X-ray coordinates.

It is characteristic of large molecules that the structure relaxes to distribute repulsive interactions, and the molecular mechanics computations reflect this characteristic. As a consequence certain terms may best be treated as summations since individual components are numerous and exhibit deviations either way.

Hydrogen bonds and related Coulombic factors account for about half of the computed D–L differences in steric energies for the transition-state models for Phe and for Trp. The remainder arises from angle and torsional distortion and from van der Waals interactions. The relative constancy of the subtotal values for Ac-Trp-X, viz., 3.3 and 3.8, shows that the pull-down force did not cause much perturbation. It is clear the computed D–L differences are relatively insensitive to quite extensive differences in the force field.

For Lock-HN (Figures 4 and 5), Coulombic effects related to the normal hydrogen bonds favor the L enantiomer. There is, however, a pronounced tendency for the L enantiomer to rise up out of the aryl pocket in order to alleviate angle and torsional distortion. If this conformational adjustment is allowed, then the van der Waals attractive forces fall off as shown by the −7.3 value in the next to last line of Table IV. If, on the other hand, the ring is constrained to the pocket by a pull-down force (Table II), then there is the compensation shown by the subtotal values in the last line. Either form of force field leads to about the same D–L difference.

There has been considerable interest in the proposal that enzymes have been designed to stabilize transition states (Pauling, 1946). A questionable extension of the concept has the enzyme exerting a Procrustean "rack" effect that tends to distort the substrate ground state in the direction of the transition-state structure. Such distortion remains a possibility for a large substrate which makes a sufficient number of contacts with an enzyme. It is, after all, a commonplace occurrence in many molecular systems for some bonds, angles, or torsions to be distorted ($+\Delta H$, relatively large) in order to minimize the overall energy [$\sum(-\Delta H)$, many of these, all small].

However, with a small leaving group, such as HN_2 in the present systems or OCH_3 for the Lock-HN example, there is no way to introduce strain (ΔH) into the scissile C–N or C–O bond without having a compensating attractive interaction ($-\Delta H$) localized at the NH_2 group. No group is available to provide this hypothetical several kilocalorie pull on NH_2 to give distortion. It is important to keep in mind that the natural role of chymotrypsin is that of an endopeptidase.

The enzyme chymotrypsin has clearly been designed to stabilize the transition state, but not in terms of van der Waals interactions that force strain into the reactant state. The reaction of an alcohol with an amide or an ester is a high-energy process (eq 2) because of the developing Coulombic

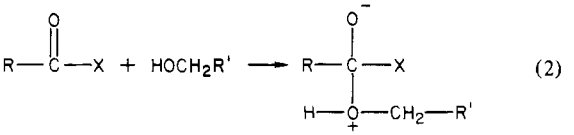

(2)

charge. Acyl transfer reactions therefore require some form of acid–base catalysis to lower this unfavorable energy (Gresser & Jencks, 1977). That the active site of chymotrypsin provides the necessary apparatus has long been recognized in terms of the imidazole ring of His_{57} as the general base and in terms of the two NH groups of Ser_{195} and Gly_{193} (Steitz et al., 1969) as general acids. The computational model has taken these important effects into account.

Calculations

The program MOLMEC adjusts internal coordinates and thus facilitates examination of the consequences of relaxing only selected structural elements (DeTar, 1977). The residues included in the model are listed in Chart I. The force constant for the anchored atoms was small enough to permit the position of the chain ends, the N of Ser_{189} and the C of Gly_{196}, to move about 0.5 Å from the X-ray position without developing excessive steric energy. The S–S bond between Cys_{191}–Cys_{220} was assigned a zero force constant in order to permit movement of the relaxed Cys_{191} away from fixed Cys_{220}. This S–S separation is defined as 1.88 Å in the X-ray coordinates and ranged from 2.1 to 2.3 Å in the runs reported in this study. Hence the maximum movement of this particular residue was about 0.4 Å. The "charge relay" system was required to maintain a plausible geometry.

The coordinates were taken from the published values (Birktoft & Blow, 1972); these differ in minor respects from the values distributed on the Brookhaven tapes (Bernstein et al., 1977). We carried out a transform to orient the active-site region so as to look directly into the aryl pocket (DeTar, 1981).

Computationally we attached each amino acid residue and the substrate separately to a set of three dummy atoms so as

to make these several groups relatively independent. Most bond lengths were held fixed. For some residues, we assigned a standard set of bond lengths, but most bonds were left at the X-ray values. We could discern no appreciable difference in results whether or not we touched up bond lengths. The imidazole ring of His_{57} and the aryl rings of the substrates were assigned standard planar geometries which were not adjusted. Torsions were adjusted about every bond (except for the fixed aryl structures), and in all critical regions torsional values were adjusted for each individual atom. Angles for the aryl rings and a few C–C–H angles of the enzyme chain were held at standard values, but nearly all angles were adjusted. Complete details are presented in the supplementary material.

The computational logistics for Ac-Trp-OCH_3 may be summarized as follows: moveable atoms 150, fixed atoms 260, parameters adjusted 189; nonbonded pairs out to 4 Å were included in adjustment (about 1400), but all 45 108 pairs were included in defining the final steric energy. The adjustments were performed in stages. A proposed starting conformation was evaluated and then subjected to about 20 iterations to ascertain whether the energy minimum was low enough to proceed. Two successive 50-iteration runs gave useful steric energies. In particular, parallel computational runs for D and L isomers showed differences that remained constant within about 0.5 kcal/mol after the first 50 iterations. The steric energies reported in Table I and II all are based on at least 250 iterations, and the energy drift per 20 iterations had dropped below 0.08 kcal. We have discovered no certain way to extrapolate the data to a reliable final energy minimum; an exponential fall-off is an approximation that consistently underestimates the drop observed on further iterations. We explored the minimization process in some detail. The status of the minimization process for the values reported in Tables I and II is shown by the results of runs of 200 further iterations on Ac-Trp-X. In comparison with the values reported in Table I, the further iterations gave the following results (kcal/mol): for L, bonded 17.47, total nonbonded −129.06, net steric energy −111.59 (a drop of 0.45 kcal/mol over the Table I value; for D, bonded 18.35, total nonbonded −122.58, net steric energy −104.23 (a drop of 0.27 kcal/mol). The D–L steric energy differences were as follows: 7.21; 100 more iterations for D, 56 for L (converged to 0.0014 kcal per iteration) gave 7.18; and 200 more on each (with lowered cut-off) gave 7.36 (an increase of 0.2 kcal). We estimate that energy differences are reliable to about 0.3 kcal and that the reported values of steric energies are within 0.5 kcal of the true minimum.

We cannot overemphasize the importance of consistency in the calculations. For example, the nonbonded sets out to 4 Å are different for L and D substrates. For Ac-Trp-OCH_3 the D–L difference in steric energies was 5.97 kcal/mol based on bonded energies plus just those nonbonded pairs included in the minimization; there were 1437 for L and 1454 for D in the final 200 iterations for this specially treated pair. Consistent sets including all nonbonded pairs gave a D–L difference of 7.36 kcal/mol. There was little change in the composition of the included set in any of the final 300 iterations. In addition to use of computer assembly of data from a common data base to ensure consistency, we routinely processed the output values by comparison programs in order to permit comprehensive inspection of all differences in geometries and in energies.

The force field is based on the Hooke's law functions for angles and for those few bonds that were adjusted. Torsional barriers were set to values similar to those we have used before (DeTar & Tenpas, 1976; DeTar et al., 1978; DeTar & Luthra, 1977, 1979, 1980; Engler et al., 1973). Nonbonded interactions used the 12/6 function. The constants are in the range of those used in other studies. At this stage of development there appears to be no agreed upon set of force-field constants (Momany et al., 1975; Hagler et al., 1976, 1979a–c). In particular, the published nonbonded functions differ appreciably. We have in almost all instances used intermediate values with respect to those published. The computations required about 12 s/iteration on the CDC Cyber 73 and required about 122 K(octal) of memory. Efficiency could no doubt be improved considerably.

Details of the force field are provided in computer output for a representative calculation. This has been submitted as supplementary material.

Conclusions

The present study has demonstrated for the first time the feasibility of computing theoretically the energies of enzyme–substrate interactions with sufficient accuracy to permit useful predictions of relative rates. The study has provided a theoretical analysis of the underlying principles and has identified enzyme systems that are particularly suitable for theoretical computation.

The study has also demonstrated that the computed differential steric energies are relatively insensitive to large variations in the force field.

The present study has necessarily concentrated on the evaluation of highly simplified models, a decision dictated by two important practical considerations. It was necessary to determine how far it is possible to go computationally with models closely related to the X-ray geometry of the active-site region having present in the aryl pocket an attached substrate–inhibitor, namely the tosyl group. It was also important to conserve computational resources since many dozens of conformational variants had to be evaluated.

However, the present model, having one side of the specificity pocket in a frozen geometry, is unrealistically simple, and the next stage will require relaxation of all residues in the neighborhood of the substrate. Preliminary computations of "free" but complexed substrate show steric energies that are comparable for several enantiomeric pairs and accord with experiment. However, the present semirigid model shows inadequate differentiation among the acyl-enzymes.

From the point of view of theoretical chemistry, the present studies represent the first attempt to compute the effects of steric orientation on relative rates of reactions. Previous successful applications of molecular mechanics to reaction kinetics have been in the computation of the other two major steric effects, namely, steric hindrance and steric acceleration.

Acknowledgments

I am indebted to Narender P. Luthra and to E. Cheng for the initial computational work. The computer programs were derived initially from the elegant but small Bartell program (Jacob et al., 1967) and the initial development was made possible through the kind generosity of J. Dunitz (ETH, Zurich), who was host during a sabbatical visit by the author.

Supplementary Material Available

Descriptions of torsion angles and details of the force field (36 pages). Ordering information is given on any current masthead page.

References

Ashworth, J., & Coller, B. A. (1971) *Trans. Faraday Soc. 67*, 1069–1077.

Bender, M. L., & Kezdy, F. J. (1964) *J. Am. Chem. Soc. 86*, 3704–3714.

Bender, M. L., & Killheffer, J. V. (1973) *Critical Reviews in Biochemistry*, The Chemical Rubber Co., Cleveland, OH.
Bender, M. L., Kezdy, F. J., & Gunter, C. R. (1964) *J. Am. Chem. Soc. 86*, 3714–3721.
Bernstein, F. C., Koetzle, T. F., Williams, G. J. B., Meyer, E. F., Jr., Brice, M. D., Rodgers, J. R., Kennard, O., Shimanouchi, T., & Tasumi, M. (1977) *J. Mol. Biol. 112*, 535–542.
Bingham, R. C., & Schleyer, P. v. R. (1971) *J. Am. Chem. Soc. 93*, 3189–3199.
Birktoft, J. J., & Blow, D. M. (1972) *J. Mol. Biol. 68*, 187–240.
Birktoft, J. J., Kraut, J., & Freer, S. T. (1976) *Biochemistry 15*, 4481–4485.
Blow, D. M. (1976a) *J. Am. Chem. Soc. 98*, 6690–6695.
Blow, D. M. (1976b) *Acc. Chem. Res. 9*, 145.
Bosshard, H. R. (1974) *Isr. J. Chem. 12*, 495–504.
Brandt, K. G., Himoe, A., & Hess, G. P. (1967) *J. Biol. Chem. 242*, 3937–3982.
Cohen, F. E., & Sternberg, M. J. E. (1980) *J. Mol. Biol. 136*, 9–22.
Cohen, G. H., Silverton, E. W., Matthews, B. W., Braxton, H., & Davies, D. R. (1969) *J. Mol. Biol. 44*, 129–141.
Cohen, S. G., & Schultz, R. M. (1968) *J. Biol. Chem. 243*, 2607–2617.
Dauber, P., & Hagler, A. T. (1980) *Acc. Chem. Res. 13*, 105–112.
Davies, D. R., Cohen, G. H., Silverton, E. W., Braxton, H., & Matthews, B. W. (1969) *Acta Crystallogr., Sect. A 25*, 5182.
DeTar, D. F. (1977) *Comput. Chem. 1*, 141–144.
DeTar, D. F. (1980a) *J. Org. Chem. 44*, 5166, 5174.
DeTar, D. F. (1980b) *J. Am. Chem. Soc. 102*, 7988.
DeTar, D. F. (1981) *J. Am. Chem. Soc. 103*, 107–110.
DeTar, D. F., & Tenpas, C. J. (1976) *J. Am. Chem. Soc. 98*, 7903–7908.
DeTar, D. F., & Luthra, N. P. (1977) *J. Am. Chem. Soc. 99*, 1232.
DeTar, D. F., & Luthra, N. P. (1979) *J. Org. Chem. 44*, 3299–3305.
DeTar, D. F., & Luthra, N. P. (1980) *J. Am. Chem. Soc. 102*, 4505–4512.
DeTar, D. F., McMullen, D. F., & Luthra, N. P. (1978) *J. Am. Chem. Soc. 100*, 2484–2493.
Engler, E. M., Andose, J. D., & Schleyer, P. v. R. (1973) *J. Am. Chem. Soc. 95*, 8005–8025.
Fastrez, J., & Fersht, A. R. (1973) *Biochemistry 12*, 2025–2034.
Finkelstein, A. V., & Ptitsyn, O. B. (1977) *Biopolymers 16*, 469–495.
Foster, R. J., & Niemann, C. (1955) *J. Am. Chem. Soc. 77*, 1886–1892.
Foster, R. J., Shine, H. J., & Niemann, C. (1955) *J. Am. Chem. Soc. 77*, 2378–2383.
Gresser, M. J., & Jencks, W. P. (1977) *J. Am. Chem. Soc. 99*, 6963–6970 (there is an extensive literature).
Hagler, A. T., & Lifson, S. (1974) *J. Am. Chem. Soc. 96*, 5327–5335.
Hagler, A. T., & Bernstein, J. (1978) *J. Am. Chem. Soc. 100*, 6349–6354.
Hagler, A. T., Huler, E., & Lifson, S. (1974) *J. Am. Chem. Soc. 96*, 5319–5327.
Hagler, A. T., Leiserowitz, L., & Tuval, M. (1976) *J. Am. Chem. Soc. 98*, 4600–4612.
Hagler, A. T., Lifson, S., & Dauber, P. (1979a) *J. Am. Chem. Soc. 101*, 5122–5130.
Hagler, A. T., Dauber, P., & Lifson, S. (1979b) *J. Am. Chem. Soc. 101*, 5131–5141.
Hagler, A. T., Stern, P. S., Sharon, R., Becker, J. M., & Naider, F. (1979c) *J. Am. Chem. Soc. 101*, 6842–6852.
Hein, G. E., & Niemann, C. (1962a) *J. Am. Chem. Soc. 84*, 4487–4494.
Hein, G. E., & Niemann, C. (1962b) *J. Am. Chem. Soc. 84*, 4495–4503.
Henderson, R. (1970) *J. Mol. Biol. 54*, 341–354.
Honig, B., Ray, A., & Levinthal, C. (1976) *Proc. Natl. Acad. Sci. U.S.A. 73*, 1974–1978.
Jacob, E. J., Thompson, H. B., & Bartell, L. S. (1967) *J. Chem. Phys. 47*, 3736–3753.
Kezdy, F. J., Clement, G. E., & Bender, M. L. (1964) *J. Am. Chem. Soc. 86*, 3690–3696.
Komiyama, M., & Bender, M. L. (1979) *Proc. Natl. Acad. Sci. U.S.A. 76*, 557–560.
Kortüm, G., Vogel, W., & Andrussow, K. (1961) *Dissociation Constants of Organic Acids in Aqueous Solution*, Butterworths, London.
Kraut, J. (1971) *Enzymes, 3rd Ed. 3* 165–183.
Kraut, J. (1977) *Annu. Rev. Biochem. 46*, 331–358.
Lesk, A. M., & Chothia, C. (1980) *J. Mol. Biol. 136*, 225–270.
Levitt, M. (1974) *J. Mol. Biol. 82*, 393–420.
Levitt, M., & Warshell, A. (1975) *Nature (London) 253*, 694–698.
Lifson, S., Hagler, A. T., & Dauber, P. (1979) *J. Am. Chem. Soc. 101*, 5111–5121.
Matthews, D. A., Alden, R. A., Birktoft, J. J., Freer, S. T., & Kraut, J. (1977) *J. Biol. Chem. 252*, 8875–8883.
McCammon, J. A., & Karplus, M. (1979) *Proc. Natl. Acad. Sci. U.S.A. 76*, 3585–3589.
Momany, F. A. (1976) *J. Am. Chem. Soc. 98*, 2990.
Momany, F. A., Carruthers, L. M., McGuire, R. F., & Scheraga, H. A. (1974a) *J. Phys. Chem. 78*, 1595–1620.
Momany, F. A., Carruthers, L. M., & Scheraga, H. A. (1974b) *J. Phys. Chem. 78*, 1621–1630.
Momany, F. A., McGuire, R. F., Burgess, A. W., & Scheraga, H. A. (1975) *J. Phys. Chem. 79*, 2361–2381.
Pauling, L. (1946) *Chem. Eng. News 24*, 1375–1377.
Pincus, M. R., Burgess, A. W., & Scheraga, H. A. (1976) *Biopolymers 15*, 2485–2521.
Platzer, K. E. B., Momany, F. A., & Scheraga, H. A. (1972a) *Int. J. Pept. Protein Res. 4*, 187–200.
Platzer, K. E. B., Momany, F. A., & Scheraga (1972b) *Int. J. Pept. Protein Res. 4*, 201–219.
Ramachandran, G. N., Ramakrishnan, C., & Sasisekharan, V. (1963) *J. Mol. Biol. 7*, 95.
Ramachandran, G. N., Lakshminarayanan, A. N., Balasubramanian, R., & Tegoni, G. (1970) *Biochim. Biophys. Acta 221*, 165.
Rodgers, P. S., Goaman, L. C. G., & Blow, D. M. (1976) *J. Am. Chem. Soc. 98*, 6690–6695.
Ruhlmann, A., Kukla, D., Schwager, P., Bartels, K., & Huber, R. (1973) *J. Mol. Biol. 77*, 417–431.
Scheraga, H. A. (1971) *Chem. Rev. 71*, 195–217.
Segal, D. M., Powers, J. C., Cohen, G. H., Davies, D. R., & Wilcox, P. E. (1971) *Biochemistry 10*, 3728–3738.
Steitz, T. A., Henderson, R., & Blow, D. M. (1969) *J. Mol. Biol. 46*, 337–348.
Thompson, A. B. (1967) *J. Chem. Phys. 47*, 3407–3410.
Tulinsky, A., Vandlen, R. L., Morimoto, C. N., Mani, N., & Wright, L. H. (1973) *Biochemistry 12*, 4185–4192.

Tulinsky, A., Mavridis, I., & Mann, R. F. (1978) *J. Biol. Chem. 253*, 1074–1078.
Vandlen, R. L., & Tulinsky, A. (1971) *Acta Crystallogr., Sect. B 27*, 437–442.
Vandlen, R. L., & Tulinsky, A. (1973a) *Acta Crystallogr., Sect. B 29*, 1309.
Vandlen, R. L., & Tulinsky, A. (1973b) *Biochemistry 12*, 4193–4200.
Venkatachalam, C. M., Price, B. J., & Krimm, S. (1974) *Macromolecules 7*, 212.
Venkatachalam, C. M., Price, B. J., & Krimm, S. (1975) *Biopolymers 14*, 1121.
Wallace, R. A., Kurtz, A. N., & Niemann, C. (1963) *Biochemistry 2*, 824–836.
White, D. N. J., & Morrow, C. (1977) *Comput. Chem. 1*, 225–233.
Zerner, B., & Bender, M. L. (1964) *J. Am. Chem. Soc. 86*, 3669–3674.
Zerner, B., Bond, R. P. M., & Bender, M. L. (1964) *J. Am. Chem. Soc. 86*, 3674–3679.

Interactions between Sarcoplasmic Reticulum Calcium Adenosinetriphosphatase and Nonionic Detergents†

William L. Dean* and Carolyn P. Suárez

ABSTRACT: The interaction of Triton X-100 and other nonionic detergents with a delipidated preparation of the Ca^{2+}ATPase from sarcoplasmic reticulum has been studied. Binding of radiolabeled Triton X-100 was determined by column chromatography at 6 °C, and two classes of binding sites were observed. Below the critical micelle concentration (cmc), binding of Triton occurred at 35–40 equivalent sites on the delipidated ATPase with a binding constant of 2.7×10^4 M^{-1}. Near the cmc cooperative binding of an additional 70 molecules of the detergent was observed. The binding of monomeric Triton X-100 below the cmc was associated with a parallel activation of over half of the ATPase activity, and the remainder of the activity was recovered after the detergent concentration was increased to the cmc. The ability to reactivate ATPase activity was more dependent on the polar poly(oxyethylene) portion of nonionic detergents than on the hydrocarbon portion. Generalizing for all amphiphiles, these results suggest that there are discrete binding sites on the Ca^{2+}ATPase for phospholipid molecules in the native membrane and that the polar head groups of phospholipids interact more strongly with the protein than the hydrophobic acyl chains. Perturbations in micelle structure were observed for several nonionic detergents by measurement of *cis*-parinaric acid fluorescence and differential scanning calorimetry, and discontinuities in Arrhenius plots occurred at the transition temperature of the detergent used for reactivation of ATPase activity. It is concluded that both the physical state of the micelle and the intrinsic behavior of the ATPase polypeptide affect the temperature dependence of ATPase activity.

The Ca^{2+}ATPase[1] from sarcoplasmic reticulum has been demonstrated to have an obligatory requirement for bound amphiphiles. In the absence of amphiphiles the ATPase cannot hydrolyze ATP, but when the appropriate phospholipids or detergents are bound, ATP hydrolysis occurs in the presence of Ca^{2+} (Martonosi, 1968; Warren et al., 1974; Dean & Tanford, 1977). The results from several different approaches have suggested that ~30 mol of phospholipid is associated with the ATPase in a phospholipid bilayer (Warren et al., 1974; Hesketh et al., 1976; le Maire et al., 1976). Since phospholipid molecules aggregate to form bilayers at very low concentrations (e.g., 4.6×10^{-10} M for dipalmitoylphosphatidylcholine; Smith & Tanford, 1972), it has not been possible to determine the affinity of phospholipid molecules for the ATPase. In fact, there is a controversy as to how the kinetics of phospholipid association is related to ATPase activity, and it has been suggested that lipid molecules may exchange during the time scale of the enzymatic turnover (Rice et al., 1979).

Because detergents have much higher cmc's than phospholipids (Tanford, 1973), they are well suited for the study of protein–amphiphile interactions. In the present report the affinity of [^{3}H]Triton X-100 for the delipidated Ca^{2+}ATPase (Dean & Tanford, 1977) is determined by a column chromatographic technique (Hummel & Dreyer, 1962). Since Triton X-100 effectively supports ATPase activity, the relationship between detergent monomer binding and activation of ATPase activity can be observed directly. Furthermore, since a wide variety of detergents of differing structure are commercially available, it is possible to assess the relative importance of the polar and nonpolar portions of detergents for supporting ATPase activity.

Another aspect of amphiphile–ATPase interaction that can be readily probed with nonionic detergents is the effect of the physical state of the amphiphile on ATPase activity. Several laboratories have reported discontinuities in Arrhenius plots of ATPase activity near 20 °C for the Ca^{2+}ATPase in its native membrane (Inesi et al., 1973; Lee et al., 1974; Dean & Tanford, 1978; Moore et al., 1978). This behavior has been attributed to a liquid-crystalline transition of the lipid closely associated with the ATPase, since the bulk lipid displays a transition at a much lower temperature (Hesketh et al., 1976; Davis et al., 1976). However, a delipidated preparation reactivated with the nonionic detergent $C_{12}E_8$ also exhibited a discontinuity near 20 °C, and the authors concluded that

† From the Department of Biochemistry, University of Louisville School of Medicine, Louisville, Kentucky 40292. *Received August 18, 1980.* This work was supported by a grant from the Muscular Dystrophy Association.

[1] Abbreviations used: $C_{12}E_8$, dodecyl octaethylene glycol monoether; cmc, critical micelle concentration; ATP, adenosine 5′-triphosphate; Ca^{2+}ATPase, calcium adenosinetriphosphatase; TES, *N*-tris(hydroxymethyl)methyl-2-aminoethanesulfonic acid.

0006-2960/81/0420-1743$01.25/0